

# Thomson scattering in a low-pressure argon mercury positive column

**Citation for published version (APA):**

Bakker, L. P., & Kroesen, G. M. W. (2000). Thomson scattering in a low-pressure argon mercury positive column. *Journal of Applied Physics*, 88(7), 3899-3904. <https://doi.org/10.1063/1.1290733>

**DOI:**

[10.1063/1.1290733](https://doi.org/10.1063/1.1290733)

**Document status and date:**

Published: 01/01/2000

**Document Version:**

Publisher's PDF, also known as Version of Record (includes final page, issue and volume numbers)

**Please check the document version of this publication:**

- A submitted manuscript is the version of the article upon submission and before peer-review. There can be important differences between the submitted version and the official published version of record. People interested in the research are advised to contact the author for the final version of the publication, or visit the DOI to the publisher's website.
- The final author version and the galley proof are versions of the publication after peer review.
- The final published version features the final layout of the paper including the volume, issue and page numbers.

[Link to publication](#)

**General rights**

Copyright and moral rights for the publications made accessible in the public portal are retained by the authors and/or other copyright owners and it is a condition of accessing publications that users recognise and abide by the legal requirements associated with these rights.

- Users may download and print one copy of any publication from the public portal for the purpose of private study or research.
- You may not further distribute the material or use it for any profit-making activity or commercial gain
- You may freely distribute the URL identifying the publication in the public portal.

If the publication is distributed under the terms of Article 25fa of the Dutch Copyright Act, indicated by the "Taverne" license above, please follow below link for the End User Agreement:

[www.tue.nl/taverne](http://www.tue.nl/taverne)

**Take down policy**

If you believe that this document breaches copyright please contact us at:

[openaccess@tue.nl](mailto:openaccess@tue.nl)

providing details and we will investigate your claim.

# Thomson scattering in a low-pressure argon mercury positive column

L. P. Bakker<sup>a)</sup> and G. M. W. Kroesen

*Department of Applied Physics, Eindhoven University of Technology, P.O. Box 513, 5600 MB Eindhoven, The Netherlands*

(Received 24 April 2000; accepted for publication 7 July 2000)

The electron density and the electron temperature in a low-pressure argon mercury positive column are determined using Thomson scattering. Special attention has been given to the stray light reduction in the Thomson scattering setup. The results are obtained in a discharge tube with a 26 mm diam, 5 mbar of argon, a mercury pressure in between 0.14 and 1.7 Pa, and an electric current ranging from 200 to 400 mA. The systematic error in the electron density is 15%, the statistical error is 25%. The total error in the electron temperature is 10%–20%. © 2000 American Institute of Physics. [S0021-8979(00)02820-6]

## I. INTRODUCTION

Knowledge of the electron density and temperature is very important in the modeling, the research, and the development of fluorescent lamps. In the past, several authors reported the determination of the electron density and temperature with the aid of a Langmuir probe.<sup>1–3</sup> The main disadvantage of these measurements is that Langmuir probes disturb the plasma at the very position the plasma quantities are being measured. Furthermore, a probe does not directly measure the electron density and temperature. In fact, what a probe measures is the reaction of the charged species in the plasma on the disturbance by the probe. Therefore, a considerable amount of theory is necessary to obtain the electron density and temperature from the probe characteristic.

In contrast to Langmuir probe measurements, incoherent Thomson scattering measurements provide us with unambiguous values of the electron density and temperature. Moreover, these measurements are nonintrusive. However, due to the very low cross section of Thomson scattering, along with the proximity of the tube wall, which results in a very high stray light level, these measurements could not be done using the standard Thomson scattering technique. In a recent article, we report Thomson scattering measurements in a fluorescent lamp.<sup>4</sup> Especially the use of an atomic vapor absorption cell that absorbs the stray light in the setup described in this article makes it possible to measure a Thomson scattering spectrum in a fluorescent lamp.

Fluorescent lamps are filled with a few hundred pascals of a mixture of noble gases, along with a tenth to a few pascals of mercury. The excited states of the mercury atom have a much lower energy than the corresponding excited states of the noble gases. Therefore, it is much easier for an electron to excite a mercury atom than to excite a noble gas atom. The electron temperature in the positive column of the discharge is limited mainly by the inelastic collisions with mercury atoms, assuming the mercury density is sufficiently high. This limitation also prohibits the excitation of the noble gas atoms. Therefore, the spectral lines of mercury dominate

the emission spectrum of the discharge. However, when the mercury density is decreased, the electrons lose less energy to the mercury atoms. Then the electron energy can increase due to the heating by the electric field. Due to this increase in the electron energy, the noble gas atoms can also be excited. The spectral lines of the noble gas can be added to the mercury spectrum. So the emission spectrum of a fluorescent lamp can be changed by controlling the mercury density in the lamp.<sup>5</sup>

This article describes the electron density and temperature measurements we performed in a fluorescent lamp under a number of different conditions. We are especially interested in the electron density and the electron temperature at a relatively low mercury pressure. Besides this, the fluorescent lamp under standard conditions is also investigated.

## II. EXPERIMENTAL SETUP

The Thomson scattering measurements are performed with the setup described in Ref. 4. The setup consists of three parts. The first part consists of an excimer pumped dye laser with an amplified spontaneous emission filter. The second part consists of a lens focusing the laser beam in front of the detection branch, the discharge lamp, and a laser power monitor. The third part is the detection branch, which consists of a spectrograph with an intensified charge-coupled device (ICCD), two lenses making an image of the laser beam on the slit of a spectrograph, and a sodium vapor absorption cell. Figure 1 shows a schematic drawing of the setup. The first part of the setup produces a laser beam with a wavelength of 589 nm and a high spectral purity. This laser beam is shone through the discharge lamp and the scattered light is captured and subsequently guided through the sodium vapor absorption cell. This scattered light is then detected by the ICCD camera, which is mounted on the spectrograph. The slit of the spectrograph is positioned parallel to the laser beam, so the image of the laser beam is parallel with the slit. The Rayleigh scattering signal and the stray light are absorbed in the sodium cell, while the Thomson

<sup>a)</sup>Electronic mail: l.p.bakker@phys.tue.nl

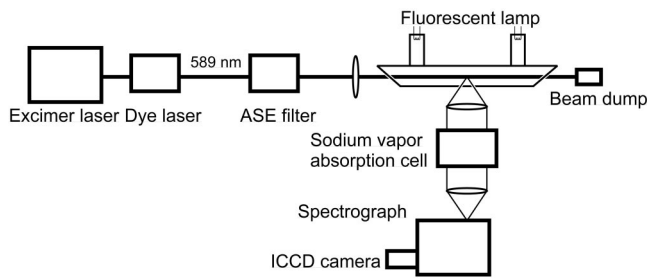


FIG. 1. Experimental setup for the Thomson scattering experiments.

scattering photons are transmitted. In this way, we obtain an efficient way of reducing the influence of stray light on the Thomson scattering spectrum.

With respect to the setup described in Ref. 4, we made some minor changes. In the detection branch, the two imaging lenses are replaced by lenses with a focal distance of 250 mm. The length of the slit is changed to 15 mm. Furthermore, the discharge lamp itself is positioned in a box with a controllable temperature, and the mercury vapor pressure in the lamp is controlled using a thermostat bath. The lamp is a U-shaped borosilicate glass tube with Brewster windows at the ends. The inner diameter of the lamp is 23.2 mm, its outer diameter is 26 mm. The argon pressure is 5 mbar. Just above the electrodes, two water jackets are positioned around the tube. With these jackets the tube is cooled locally. The temperature of these cold spots imposes the mercury vapor pressure in the tube. The water jackets are connected to a Haake FE thermostat bath. A schematic drawing of the discharge lamp is shown in Fig. 2. The discharge is sustained by a standard Philips BRC 411/01 35 kHz ballast.

The Thomson scattering setup is aligned by measuring the rotational Raman scattering spectrum in nitrogen. This spectrum is also used for the intensity calibration of the Thomson scattering measurements. The Raman scattering spectra are taken using a tube filled with 900 mbar of nitrogen. This tube is similar to the discharge tube. After the alignment of the setup is performed, the nitrogen tube is replaced by the discharge tube, leaving the rest of the setup unchanged. The laser power is measured with an Ophir AN/2 laser power monitor. The laser power used for the Thomson scattering spectra was approximately 1 W at a repetition rate of 150 Hz. We integrated the Thomson scattering spectrum for 30 min in order to improve the signal-to-noise ratio. The ICCD camera was used in the gated mode and the gate width was 300 ns. The ICCD camera is read out in the full vertical binning mode. Besides this, along the horizontal (wavelength) axis the camera is read out per three pixels. The width of the

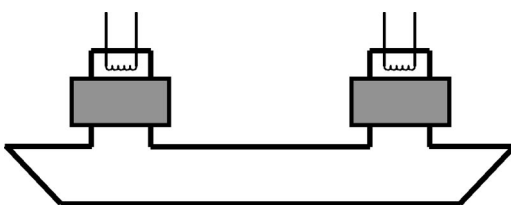


FIG. 2. Schematic drawing of the discharge lamp. The gray rectangles represent the water jackets.

TABLE I. Experimental conditions in series A, B, and C.

Series	A	B	C
Cold-spot temperatures	18	18, 40	18–50
Mercury pressure (Pa)	0.14	0.14, 0.85	0.14–1.76
Current (mA)	200, 300, 400	200–400	400
Measured quantities	$n_e(r)$ , $T_e(r)$	$n_e(0)$ , $T_e(0)$	$n_e(0)$ , $T_e(0)$

response of the camera to a single photoelectron event is also three pixels. The discharge was stable enough to allow us to perform the plasma emission measurements after the Thomson scattering spectrum is obtained. This plasma emission is measured under the same experimental conditions as the Thomson scattering spectrum. The stray light spectrum is also obtained for every Thomson scattering measurement.

The net Thomson scattering spectrum is obtained by subtracting the plasma emission and the stray light from the raw Thomson scattering spectrum. The absolute intensity is obtained using the Raman scattering spectrum, which is performed before every Thomson scattering measurement. The Thomson scattering spectrum is then fitted using a Gaussian profile for the electron velocity distribution function. The fit is obtained using a least-squares method. In the fitting procedure we only used the wings of the profile. From the fit, we obtain the electron density and the electron temperature.

The measurements are performed in three series. Table I shows the experimental conditions in each series. Series A is performed at a cold-spot temperature of 18 °C. This temperature corresponds to a mercury vapor pressure of 0.14 Pa. The electrical current through the lamp was 200, 300, and 400 mA. In this series, the radial profiles of the electron density and the electron temperature are measured. Series B is performed at the cold-spot temperatures of 18 and 40 °C. The cold-spot temperature of 40 °C corresponds to a mercury vapor pressure of 0.85 Pa. The dependency on the electrical current through the lamp is obtained between the currents 200 and 400 mA. The electron density and the electron temperature are measured at the tube axis. Series C is performed at cold-spot temperatures between 18 and 50 °C. The cold-spot temperature of 50 °C corresponds to a mercury vapor pressure of 1.76 Pa. The electrical current through the lamp was 400 mA. The electron density and the electron temperature are measured at the tube axis.

In a separate experiment, we measured the temperature of the outer tube wall at the position where the Thomson scattering spectra are measured. These temperature measurements are done for the conditions of series A, B, and C.

### III. RESULTS

The measurements are performed as described in the preceding section. An example of a measured Thomson scattering spectrum is shown in Fig. 3. The fit of the spectrum is also shown in Fig. 3. For the fit, we used a Maxwellian electron velocity distribution function, the measured transmission of the sodium vapor absorption cell, and the apparatus profile of the spectrograph. This apparatus profile is not exactly known. This is due to the fact that the width of the

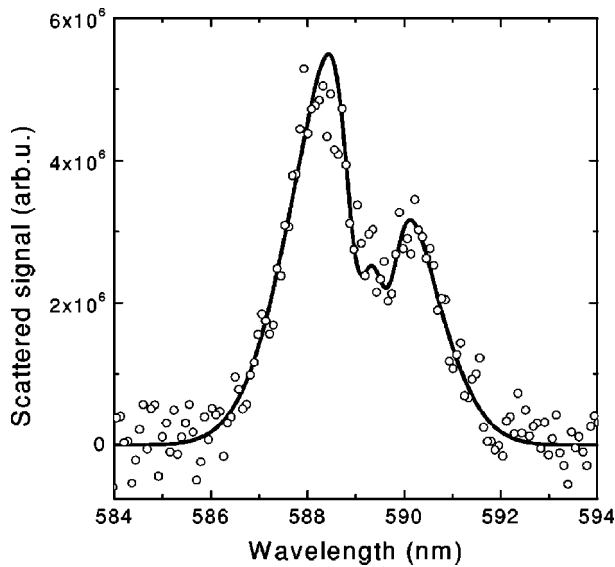
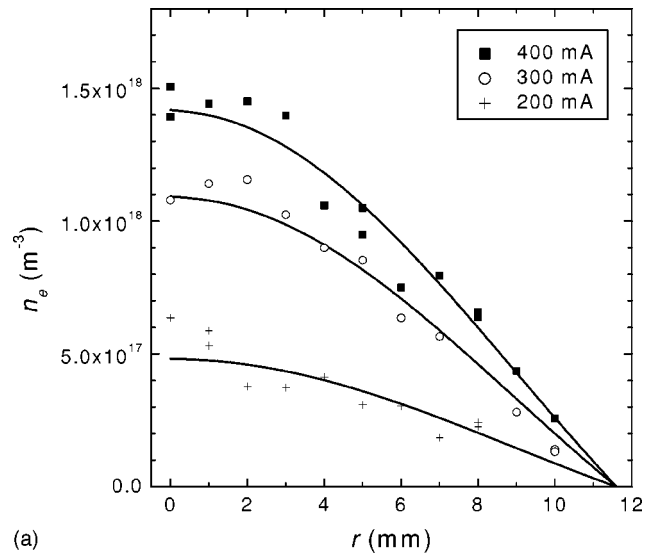


FIG. 3. Example of a Thomson scattering spectrum.

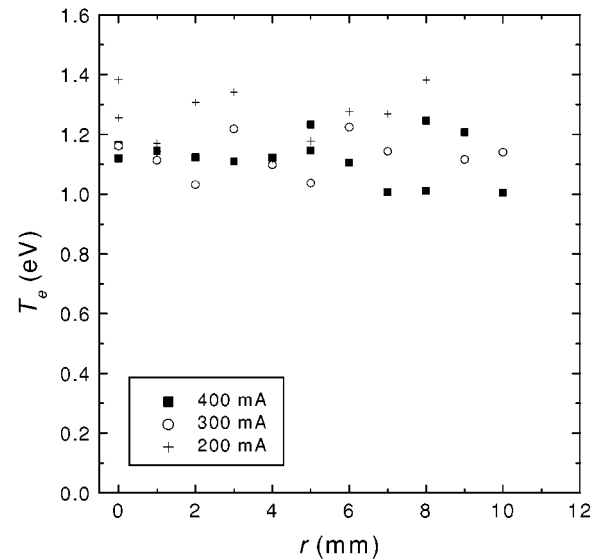
slit has been chosen larger than the image of the laser beam in the slit in order to avoid artifacts by minor misalignment. Therefore, the fit deviates from the measurement in the vicinity of the absorption lines of sodium at 589 and 589.6 nm. Furthermore, it is clear that the fit is good in the wings of the Thomson scattering profile. We fitted the measurements in the wavelength regions from 586.5 to 587.8 nm and from 590.9 to 591.4 nm. These regions correspond to the energy ranges from 0.5 to 2.3 eV and from 1.4 to 2.2 eV, respectively. The electron density and temperature resulting from the fit in Fig. 3 are  $1.0 \times 10^{18} \text{ m}^{-3}$ , and 0.94 eV, respectively.

Figure 4 shows the results of the measurement series A. The electron density and the electron temperature are plotted as a function of the radial position  $r$ . The drawn lines are Bessel profiles, fitted to the electron density measurements. The zero-order Bessel function is the diffusion solution according to the Schottky theory. From Fig. 4, it is clear that the electron density profile is approximately a Bessel function of the radial position. It is also clear that, within the experimental uncertainty, the electron temperature is not dependent on the radial position. We note that the measurements at the radial position of 10 mm are very difficult to obtain. The electron density is very low, and the stray light level is extremely high. On the one hand, the scattering of the laser beam at the tube wall is very high, the laser beam could be seen very clearly with the naked eye. On the other hand, the Thomson scattering signal contains on the average only one photon per laser pulse.

For series B we only measured the electron properties at the tube axis, i.e., at  $r=0$ . The dependency on the current  $I$  is investigated. Figure 5 shows the results of these measurements. The electron density is proportional to the current through the lamp. The electron temperature decreases with increasing current. This decreasing electron temperature is due to the multistep ionization of mercury, which starts becoming important at higher electron densities. The multistep processes allow the electron energy to decrease since the energy difference to overcome by the electrons decreases.



(a)

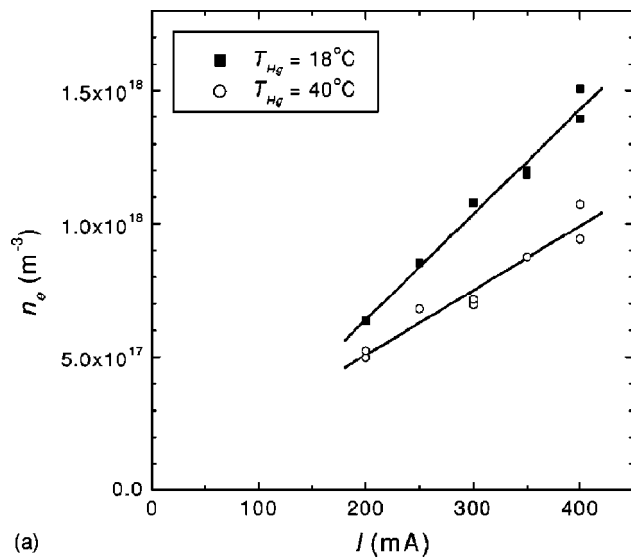


(b)

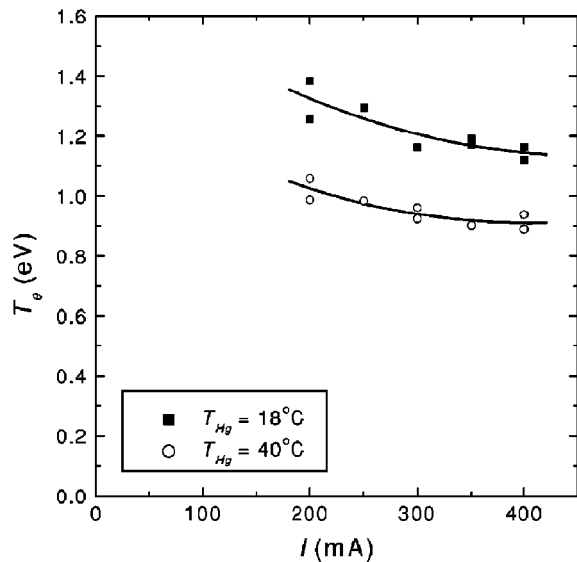
FIG. 4. (a) Electron density as a function of the radial position (series A). (b) Electron temperature as a function of the radial position.

The results of measurement series C are shown in Fig. 6. The electron density and the electron temperature both decrease with increasing cold spot temperature  $T_{\text{Hg}}$ . This is due to the increasing influence of mercury in the ionization and excitation processes. This increasing influence is clear in the emission spectrum of the discharge, as can be seen in Fig. 7, where the emission of the 585.925 nm line of mercury and the emission of the 603.213 nm line of argon is plotted as a function of the cold-spot temperature.

The outer wall temperature of the discharge tube at the position where the Thomson scattering spectra are obtained is plotted in Fig. 8, for series A, B, and C. Note that series A is measured without increasing the ambient temperature, this series is taken at an ambient temperature of 27 °C. Series B is taken at an ambient temperature of 48 °C. Series C is taken at an ambient temperature of 48 °C, except for the measurements at 45 and 49.5 °C, these were taken at an ambient temperature of 69 °C.

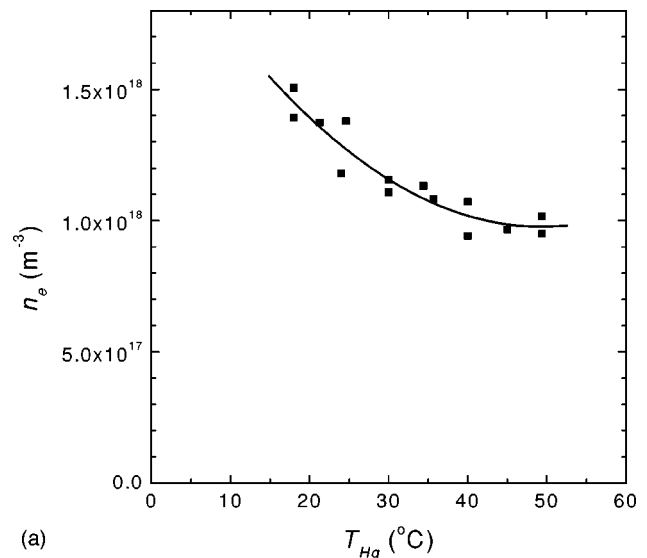


(a)

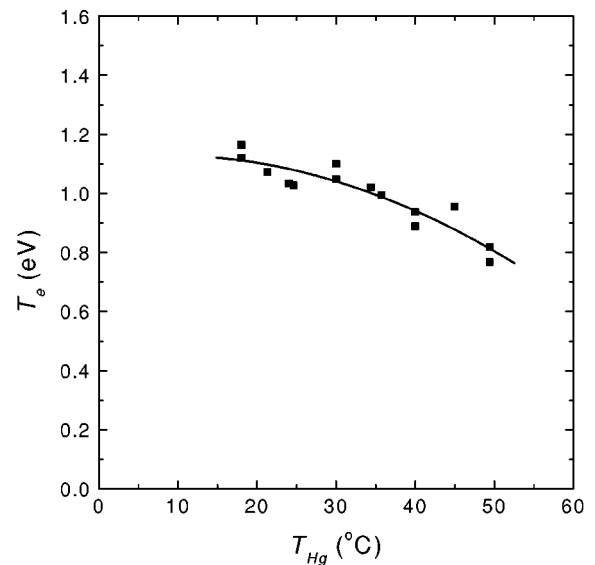


(b)

FIG. 5. (a) Electron density as a function of the current (series B). (b) Electron temperature as a function of the current.



(a)



(b)

FIG. 6. (a) Electron density as a function of the cold-spot temperature (series C). (b) Electron temperature as a function of the cold-spot temperature.

#### IV. DISCUSSION

The accuracy in the measurements is limited by systematic and a statistical errors. Systematic errors reduce the accuracy of the absolute value of the measured quantities, while the statistical errors reduce the reproducibility of the results. We will start with the discussion of the error in the electron density followed by an analysis of the error in the electron temperature.

##### A. Electron density

The absolute value of the electron density is dependent on the theoretical cross section used for rotational Raman scattering. In Ref. 4, we give an extended discussion on this cross section and the intensity calibration procedure. The error in the cross section is 8%. The uncertainty in the nitrogen pressure in the tube is approximately 10%. The error this uncertainty introduces is, however, reduced since we compared the nitrogen tube measurement to rotational Raman

measurements in air. These errors result in a total error in the absolute value of the electron density of approximately 15%. In addition to the systematic error, we introduce a statistical error, i.e., noise in the experiment itself. The first source is the power monitor reading in the Raman and Thomson scattering experiments. The inaccuracy of the power measurements is estimated to be 5%. The second source is the noise on the plasma emission, which causes an additional error, since it determines the base line of the Thomson spectra. This inaccuracy is estimated to be a few percent. The last source is the alignment of the setup. Misalignment introduces an error, since small changes in the position of the laser beam result in a different transmission of the detection branch. This inaccuracy is estimated to be 15% at maximum. The misalignment is checked after each measurement by performing a second Raman scattering experiment. The total statistical error in the electron density measurements adds up

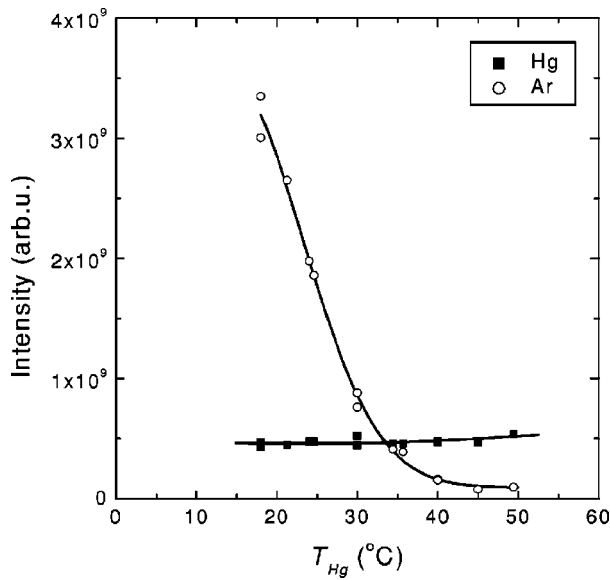


FIG. 7. Emission of the 585.925 nm line of mercury and the emission of the 603.213 line of argon as a function of the cold-spot temperature.

to roughly 25%. This relative inaccuracy is, however, reduced by measuring more than one spectrum at the same experimental conditions.

**B. Electron temperature**

The systematic error in the absolute value of the electron temperature is negligible compared to the experimental noise. The influence of the apparatus profile is in the order of 1%. Furthermore, the wavelength axis could be calibrated very precisely. The experimental noise in the electron temperature is caused by two factors. At first, the low amount of Thomson scattering photons results in a low signal-to-noise ratio per wavelength interval. Second, the influence of the

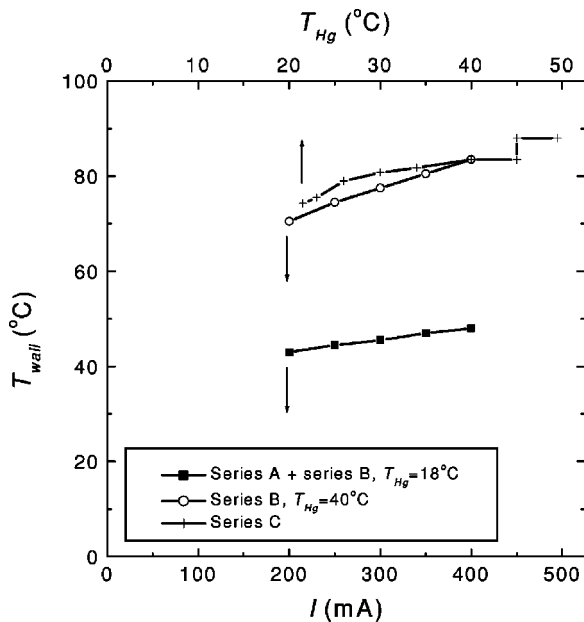


FIG. 8. Outer wall temperature of the tube for series A, B, and C.

TABLE II. Comparison between the present values for the electron density and electron temperature and the values found in the literature.

$T_{Hg}(^{\circ}C)$	$p_{Ar}(Pa)$	$I(mA)$	$n_e(m^{-3})$	$T_e(eV)$	Ref.
42	333	400 (dc)	$6.2 \times 10^{17}$	1.5	3
42	400	400 (dc)	$8.0 \times 10^{17}$	1.1	2
40	500	400 (rms 35 kHz)	$1.0 \times 10^{18}$	0.9	This work

plasma emission is not negligible in the structure of the Thomson scattering spectra. Especially the presence of spectral lines of argon and mercury that overlap the Thomson spectra is important. The total error in the electron temperature measurements is in the order of 10%–20%.

Comparison of the present results with the Langmuir probe measurements performed in the past is hard since the discharge conditions are not the same. Verweij<sup>1</sup> performed an extensive survey of an argon mercury discharge at several currents, argon pressures, and mercury pressures. The inner diameter of his discharge lamps was 36 mm, which is significantly different from the 23.2 mm we have. Denneman *et al.*<sup>2</sup> investigated the argon mercury discharge with an inner diameter of 24 mm. However, the argon pressure in their discharge tubes was 400 Pa, which is different from the 500 Pa we have. Wani<sup>3</sup> determined the electron energy distribution function in an argon mercury discharge with an inner diameter of 24 mm. The argon pressure in their discharge tubes was 333 Pa, which is also different from the 500 Pa we have. Table II gives a summary of the results of the measurements of Denneman and Wani, and compares them to our results.

It is clear that the deviation of our electron density and temperature from the values obtained by Denneman and Wani is caused by the higher argon pressure in our discharge. The same trend as a function of the argon pressure is already observed by Verweij.<sup>1</sup>

As a concluding remark, we note that the electron temperature we observe is the electron temperature in the energy region from 0.5 to 2.3 eV. In this region, the measurements could be fitted very well using a Maxwellian velocity distribution function. Outside this region, the experimental noise was too high to make any comment on the question whether or not the electron velocity distribution function is Maxwellian. The effect of depletion of the energetic tail of the electron energy distribution function is expected to be significant above the electron energy of 4.6 eV. This is the energy of the first excited state of mercury. The depletion should be well pronounced in the Thomson scattering spectrum outside the 585.5–592.5 nm region. However, at this moment we are not able to measure the electron velocity distribution function in this region (see Fig. 3).

**ACKNOWLEDGMENTS**

This research is supported by the Technology Foundation STW and Philips Lighting Eindhoven. The authors are very grateful for the valuable technical assistance of J. M. Frieriks.

<sup>1</sup>W. Verweij, Philips Res. Rep., Suppl. **2**, 1 (1961).

<sup>2</sup>J. M. Denneman, J. J. de Groot, A. G. Jack, and F. A. S. Ligthart, J. Illum. Eng. Soc. **10**, 2 (1980).

<sup>3</sup>K. Wani, J. Appl. Phys. **67**, 6130 (1990).

<sup>4</sup>L. P. Bakker, J. M. Freriks, F. J. de Hoog, and G. M. W. Kroesen, Rev. Sci. Instrum. **71**, 2007 (2000).

<sup>5</sup>L. P. Bakker and G. M. W. Kroesen, Appl. Phys. Lett. **76**, 1528 (2000).